

Requirement of the Human GARP Complex for Mannose 6-phosphate-receptor-dependent Sorting of Cathepsin D to Lysosomes

F. Javier Pérez-Victoria, Gonzalo A. Mardones, and Juan S. Bonifacino

Cell Biology and Metabolism Program, National Institute of Child Health and Human Development, National Institutes of Health, Bethesda, MD 20892

Submitted November 29, 2007; Revised February 26, 2008; Accepted March 19, 2008

Monitoring Editor: Jean Gruenberg

The biosynthetic sorting of acid hydrolases to lysosomes relies on transmembrane, mannose 6-phosphate receptors (MPRs) that cycle between the TGN and endosomes. Herein we report that maintenance of this cycling requires the function of the mammalian Golgi-associated retrograde protein (GARP) complex. Depletion of any of the three GARP subunits, Vps52, Vps53, or Vps54, by RNAi impairs sorting of the precursor of the acid hydrolase, cathepsin D, to lysosomes and leads to its secretion into the culture medium. As a consequence, lysosomes become swollen, likely due to a buildup of undegraded materials. Missorting of cathepsin D in GARP-depleted cells results from accumulation of recycling MPRs in a population of light, small vesicles downstream of endosomes. These vesicles might correspond to intermediates in retrograde transport from endosomes to the TGN. Depletion of GARP subunits also blocks the retrograde transport of the TGN protein, TGN46, and the B subunit of Shiga toxin. These observations indicate that the mammalian GARP complex plays a general role in the delivery of retrograde cargo into the TGN. We also report that a Vps54 mutant protein in the Wobbler mouse strain is active in retrograde transport, thus explaining the viability of these mutant mice.

INTRODUCTION

Lysosomal acid hydrolases are a structurally diverse group of enzymes that are efficiently targeted to mammalian lysosomes by virtue of a shared posttranslational modification: the acquisition of mannose 6-phosphate residues on their N-linked carbohydrate chains (Kornfeld and Mellman, 1989). This modification is catalyzed by the sequential action of two enzymes, a UDP-*N*-acetylglucosamine:lysosomal enzyme *N*-acetylglucosamine-1-phosphotransferase localized to *cis*-Golgi cisternae (Lazzarino and Gabel, 1988) and an *N*-acetylglucosamine-1-phosphodiester-*N*-acetylglucosaminidase localized to the *trans*-Golgi network (TGN; Rohrer and Kornfeld, 2001). At the TGN, the mannose 6-phosphate-modified hydrolases bind to two transmembrane mannose 6-phosphate receptors (MPR), a cation-dependent MPR (CD-MPR) and a cation-independent MPR (CI-MPR), leading to the concentration of the hydrolases within clathrin-coated areas of the TGN (Ghosh *et al.*, 2003). Transport carriers then form that deliver the hydrolase-MPR complexes into endosomes. Exposure to the acid pH of the endosomal lumen causes the release of the hydrolases from the MPRs, after which the hydrolases continue on to lyso-

somes while the receptors are retrieved to the TGN to be reutilized in further rounds of hydrolase sorting (Ghosh *et al.*, 2003).

It is now well established that sorting of the hydrolase-MPR complexes at the TGN involves recognition of specific signals in the cytosolic tails of the receptors by the clathrin-associated, GGA proteins and AP-1 complex (Ghosh *et al.*, 1998; Bonifacino, 2004; Ghosh and Kornfeld, 2004). The subsequent retrieval of unoccupied MPRs from endosomes to the TGN, on the other hand, depends on other components of the protein trafficking machinery. Among these are Rab9 and TIP47, which retrieve MPRs from late endosomes (Diaz and Pfeffer, 1998; Carroll *et al.*, 2001), and epsinR (Saint-Pol *et al.*, 2004) and the retromer complex (Arighi *et al.*, 2004; Seaman, 2004; Carlton *et al.*, 2005b), which do so from early endosomes or early-late endosomal intermediates. In the case of retromer, retrograde transport involves passage through tubules that emanate from the vacuolar part of endosomes (Arighi *et al.*, 2004; Carlton *et al.*, 2004, 2005a,b).

Despite the identification of several key components of the lysosomal transport machinery in mammalian cells, there is reason to think that many more components remain to be identified. Indeed, more than 60 different vacuolar protein-sorting (VPS) gene products have been shown to participate in the sorting of acid hydrolases to the vacuole of the yeast, *Saccharomyces cerevisiae* (Bowers and Stevens, 2005). The phylogenetic conservation of the core trafficking machinery and the diversification of lysosome function in mammalian cells predict that an even larger number of proteins must be involved in sorting acid hydrolases to lysosomes.

To identify novel or uncharacterized proteins that are involved in acid hydrolase sorting in human cells, we performed an RNA interference (RNAi) screen for the requirement of 39 candidate proteins in this pathway. These candi-

This article was published online ahead of print in *MBC in Press* (<http://www.molbiolcell.org/cgi/doi/10.1091/mbc.E07-11-1189>) on March 26, 2008.

Address correspondence to: Juan S. Bonifacino (juan@helix.nih.gov).

Abbreviations used: CatD, cathepsin D; MPR, mannose 6-phosphate receptor; CI-MPR, cation-independent MPR; TGN, *trans*-Golgi network; GARP, Golgi-associated retrograde protein; Vps, vacuolar protein sorting; STxB, B subunit of Shiga toxin; TEN, tubular endosomal network.

genes were selected based on their homology to yeast VPS gene products or their involvement in other endocytic or lysosomal targeting events. This screen revealed a key role for the human homolog of the yeast Golgi-associated retrograde protein (GARP; Conibear and Stevens, 2000) or Vps fifty-three (VFT; Siniouoglou and Pelham, 2001) complex in the sorting of the acid hydrolase, cathepsin D (CatD), to lysosomes. RNAi-mediated depletion of GARP subunits caused secretion of unprocessed CatD into the culture medium due to impaired recycling of MPRs from endosomes to the TGN. We also found that GARP depletion blocked endosome-to-TGN transport of the TGN protein, TGN46, and the B-subunit of Shiga toxin (STxB). In the absence of GARP, all of these proteins accumulated in a population of small vesicles that likely correspond to endosome-to-TGN retrograde transport intermediates. Finally, we observed that a missense mutation in the GARP-Vps54 subunit found in the Wobbler motor neuron disease mouse strain does not preclude its function in retrograde transport of the CI-MPR. This explains why, unlike mice with ablation of the Vps54 gene, Wobbler mice are viable. These findings thus identify the GARP complex as a novel component of the molecular machinery involved in retrograde transport of various cargo proteins in human cells, probably by enabling the fusion of endosome-derived transport carriers with the TGN.

MATERIALS AND METHODS

Recombinant DNA Procedures

GARP subunit cDNAs were amplified by PCR from human or mouse fetal brain cDNA libraries or by RT-PCR from HeLa cell total RNA. The resulting cDNAs were subsequently cloned in-frame with the V5 and hexahistidine tags at their C-termini in TOPO pEF6-V5-His (Invitrogen, Carlsbad, CA). Primer sequences are shown in the Supplementary Methods section. The mouse Vps54 cDNA was further subcloned into the XhoI-BamHI sites of pEGFP-N1 (Clontech Laboratories, Mountain View, CA). To obtain a small interfering RNA (siRNA)-resistant human Vps52-V5, five of the nucleotides targeted by the siRNA (232-GTAGATCTCCgcaTAcT-250) were mutated (232-GTAGATCTCCGcgcaTAcT-250) by site-directed mutagenesis using the QuikChange kit (Stratagene, La Jolla, CA). Mouse Vps54-V5 was also mutated at codons for D145E and I151T to match them with the human epitope selected for the generation of rabbit polyclonal antibodies. To create an allele similar to that of the Wobbler mouse, we introduced the L967Q mutation in the mouse Vps54-V5 and Vps54-GFP plasmids.

RNAi

RNAi was performed using siRNAs from Dharmacon (Lafayette, CO). Initial screens were performed with siGENOME SMART pools or ON-TARGET plus SMART pools. Subsequently, the four different duplexes of each SMART pool for GARP subunits were tested and oligonucleotides Vps52.1 (GUAGAUCUCCGUCACUAAUUU, D-011806-01), Vps53.4 (GGAUGUAAGUCUGAUUGAAUU, J-017048-08), Vps54.3 (UCACGAUGUUUGCAGUUAUU, J-021174-07, targeting only human Vps54), and Vps54.4 (CCAGAUCUCUUACGUUCAUU, J-021174-08, targeting both human and mouse Vps54) were selected and used in knockdown (KD) experiments. Transfection of oligonucleotides (typically 40 nM) was done using Oligofectamine (Invitrogen) according to the manufacturer's protocol.

Cell Transfection and Immunoprecipitation

Human HeLa epithelial or H4 neuroglioma cells (American Type Culture Collection, Manassas, VA) were cultured on 24- or 6-well plates at 37°C in DME/high-glucose medium (Invitrogen) supplemented with 10% (vol/vol) FBS, 100 U/ml penicillin, and 100 µg/ml streptomycin. When cells reached 80% confluency, they were transfected with 0.8–3.2 µg plasmids using Lipofectamine 2000 (Invitrogen) according to the manufacturer's instructions. For stable expression of Vps54-GFP in H4 cells, cells were transfected and selected in medium containing 0.5 mg/ml G418 (Geneticin, Invitrogen). Positive clones were identified by expression of Vps54-GFP by fluorescence microscopy and expanded. For immunoprecipitation experiments, cells were lysed in 50 mM Tris-HCl, pH 7.5, 150 mM NaCl, 10% glycerol, 5 mM EDTA, 1% (vol/vol) Triton X-100, and a protease inhibitor cocktail (Roche Applied Science, Indianapolis, IN), on ice for 30 min, and microcentrifuged. Lysates were further cleared with 30 µl protein A-Sepharose beads (Amersham Biosciences), before adding specific antibodies (2 µl sera) bound to protein A-Sepharose beads and rocking at 4°C for 2 h. Immunoprecipitated material

was washed three times in PBS and eluted from the beads by heating at 90°C for 3 min in Laemmli sample buffer. Samples were subsequently analyzed by SDS-PAGE and immunoblotting.

Antibodies

Polyclonal antibodies were raised by immunization of rabbits with peptides corresponding to amino acids 79–96 of human Vps52, 61–78 of human Vps53, and 138–155 of human Vps54 (Quality Controlled Biochemicals, Hopkinton, MA). Polyclonal antibodies to human Vps53 were purified by affinity chromatography on immobilized peptide. The three antibodies were able to immunoprecipitate the corresponding proteins. Only antibodies to Vps52 and Vps53 worked by immunoblotting, and none detected the endogenous proteins by immunofluorescence microscopy. In addition, the following antibodies were used for immunofluorescence and/or immunoblotting: mouse monoclonal antibodies to the V5 epitope (Invitrogen); p230 (golgin-245), Vti1a, GS28, BiP, and actin (BD Biosciences); CI-MPR (clone 2G11; AbCam, Cambridge, MA); TfR (clone H68.4; Invitrogen) and CD63 (clone H5C6; Developmental Studies Hybridoma Bank, Iowa City, IO). Rabbit polyclonal antibodies to human SNX2 (Haft *et al.*, 2000), p230 (Yoshino *et al.*, 2005), and CI-MPR (Kametaka *et al.*, 2005) have been described previously. Other polyclonal antibodies used were sheep antibody to human TGN46 (Serotec, Raleigh, NC); rabbit antibody to giantin (Covance Research Products, Denver, PA), GFP (Invitrogen), and CatD (Calbiochem, San Diego, CA); Alexa-488- or -594-, or -647-conjugated donkey anti-mouse IgG, Alexa-488- or -594-, or -647-conjugated donkey anti-rabbit IgG, and Alexa-488-, -594-, or -647-conjugated donkey anti-sheep IgG (Molecular Probes, Eugene, OR); horseradish peroxidase-conjugated mouse anti-goat IgG (Pierce, Rockford, IL); and horseradish peroxidase-conjugated donkey anti-mouse and donkey anti-rabbit IgG (Amersham Biosciences).

Immunofluorescence Microscopy

Immunofluorescence microscopy was performed as described previously (Mardones *et al.*, 2007). Fluorescently labeled cells were examined using an inverted confocal laser scanning microscope (model LSM 510; Carl Zeiss MicroImaging, Thornwood, NY) equipped with Ar, HeNe, and Kr lasers and a 63× 1.4 NA objective. Alexa-488, -594, and -643 fluorescence was visualized using excitation filters at 488, 543, and 633 nm and emission filters at 505–530, 560–605, and 605 nm, respectively. Where indicated, an epifluorescence Zeiss microscope (Carl Zeiss MicroImaging) equipped with a PlanApo 63× 1.4 NA oil immersion objective and a charge-coupled device (CCD) AxioCam MRn camera (Carl Zeiss MicroImaging) was also used.

CI-MPR Antibody and Shiga Toxin B Subunit Internalization Assays

Antibody uptake assays were carried out by incubation for 1 h at 37°C of HeLa cells grown on coverslips in the presence of 10 µg/ml mAb to the luminal domain of the CI-MPR diluted in DMEM, 1% BSA, and 25 mM HEPES, pH 7.4. The cells were washed in PBS, chased in complete medium for 1 h, washed again in PBS, and fixed in –20°C methanol. Cy3-STxB (a kind gift from L. Johannes, Curie Institute, Paris, France) was added to cells grown on coverslips at a dilution of 0.5 µg/ml in DMEM, 1% BSA, and 25 mM HEPES, pH 7.4, for 15 min at 37°C. Cells were washed in PBS and chased for 1 h at 37°C in complete medium before fixation in 3.7% paraformaldehyde.

Electrophoresis and Immunoblotting

SDS-PAGE and electroblotting onto nitrocellulose membranes were performed using the NuPAGE Bis-Tris Gel system (Invitrogen), according to the manufacturer's instructions. Incubations with primary and secondary antibodies, enzymatic detection, and quantification were performed as described (Mardones *et al.*, 2007).

Metabolic Labeling and Immunoprecipitation

Metabolic labeling of cells was carried out as described (Mardones *et al.*, 2007). Briefly, cells grown on six-well plates were pulse-labeled for 2 h at 20°C using 0.1 mCi/ml [³⁵S]methionine-cysteine (Express Protein Label; Perkin Elmer-Cetus, Boston, MA) and chased for 1–20 h at 37°C in regular medium supplemented with 0.06 mg/ml methionine and 0.1 mg/ml cysteine. Chase medium was saved for further use, and cells were rinsed twice in PBS and subjected to lysis in 50 mM Tris-HCl, pH 7.5, 150 mM NaCl, 10% glycerol, 2 mM EDTA, 1% (vol/vol) Triton X-100, and a complete protease inhibitor cocktail (Roche Applied Science). Both cell extracts and media were immunoprecipitated and analyzed by SDS-PAGE and fluorography. Quantification was performed on a Typhoon 9200 PhosphorImager (Amersham Biosciences) using ImageQuant analysis software.

Glycerol Gradient Centrifugation

Subcellular fractionation on glycerol gradients was performed as described (Zolov and Lupashin, 2005) with slight modifications. Briefly, siRNA-treated HeLa cells from one 6-cm plate were collected in PBS-0.5 mM EDTA, pelleted by centrifugation for 5 min at 500 × g, washed once in PBS and once in STE

buffer (250 mM sucrose, 20 mM Tris-HCl, pH 7.4, 1 mM EDTA, with protease inhibitors), homogenized by 20 passages through a 25-gauge needle in 0.5-ml buffer STE without sucrose, and then centrifuged at $1000 \times g$ for 2 min to obtain a postnuclear supernatant (PNS). PNS (0.6 ml) was layered on top of a 2%-stepwise, 10–30% (wt/vol) glycerol gradient (11 ml in 20 mM Tris-HCl, pH 7.4, and 1 mM EDTA on a 0.4 ml 80% sucrose cushion) and centrifuged at $280,000 \times g$ for 60 min in a SW40 Ti rotor (Beckman Coulter, Fullerton, CA). Fractions (0.9 ml) were collected from the top. All steps were performed at 4°C. Aliquots of 0.3 ml from each fraction were precipitated with trichloroacetic acid, resuspended in Laemmli sample buffer, and analyzed by SDS-PAGE and immunoblotting.

RESULTS

An RNAi Screen Implicates Human *Vps52* in the Biosynthetic Sorting of *CatD* to Lysosomes

To identify novel components of the molecular machinery involved in the sorting of acid hydrolase precursors to lysosomes, we conducted a small-scale RNAi screen in HeLa cells using siRNAs directed to 39 candidate proteins (listed in legend to Figure 1). Among the candidate proteins were the human orthologues of several yeast VPS gene products that had not been well characterized in mammals. Cells treated with the different siRNAs were analyzed by immunofluorescence microscopy for the distribution of the acid hydrolase, *CatD*. In control cells, *CatD* exhibited its characteristic localization to lysosomes that were scattered throughout the cytoplasm (Figure 1A) and contained the tetraspanin, CD63 (Figure 1B). Although treatment with several siRNAs altered this distribution (data not shown), by far the biggest change was seen for cells treated with siRNAs targeting the human ortholog of yeast *Vps52* (Figure 1, D–F). These cells exhibited greatly reduced staining for *CatD* (Figure 1D) as well as enlargement and clustering of lysosomes stained for CD63 (Figure 1E). The residual *CatD* staining in *Vps52*-depleted cells did not colocalize with CD63 but appeared restricted to the Golgi area (Figure 1F).

To determine whether the altered *CatD* staining in *Vps52*-depleted cells was due to biosynthetic missorting, we per-

formed pulse-chase analysis of cells that were metabolically labeled with [³⁵S]methionine-cysteine for 2 h at 20°C (to arrest transport at the TGN) and then incubated in complete medium for different periods at 37°C (to allow release of *CatD* from the TGN). *CatD* species were isolated by immunoprecipitation from both cell extracts and culture media and resolved by SDS-PAGE and fluorography (Figure 1G). We observed that, in control cells, the ~50-kDa *CatD* precursor (p) was cleaved to a ~47-kDa intermediate (i) and, subsequently, to a ~31-kDa mature (m) form over a period of 3–5 h (Figure 1G). This proteolytic processing of the precursor reflects the transport of the protein to lysosomes. A fraction of the precursor was secreted intact into the medium (Figure 1G), as is known to occur in transformed cells such as HeLa. Interestingly, in *Vps52*-siRNA-treated cells, appearance of the intermediate form was delayed and the mature form was undetectable even after 5 h of chase (Figure 1G). In addition, secretion of intact precursor increased about fivefold (Figure 1G). From these experiments we concluded that depletion of *Vps52* caused severe missorting of the *CatD* precursor.

Human *Vps52* Is a Component of the GARP Complex

Vps52 was first identified in yeast as a component of the peripheral membrane protein complex known as GARP (Conibear and Stevens, 2000) or VFT (Siniosoglou and Pelham, 2001) complex. In addition to *Vps52*, the yeast complex comprises two other subunits named *Vps53* and *Vps54*, and a more loosely associated component named *Vps51* (Conibear and Stevens, 2000; Siniosoglou and Pelham, 2002; Conibear *et al.*, 2003; Reggiori *et al.*, 2003). A similar complex has recently been described in humans (Liewen *et al.*, 2005), with the notable difference that no *Vps51* homolog has yet been identified in humans or other mammals. To build a set of reagents that would allow us to investigate the involvement of other subunits of the human GARP complex in *CatD* sorting, we made cDNA constructs encoding human *Vps52*,

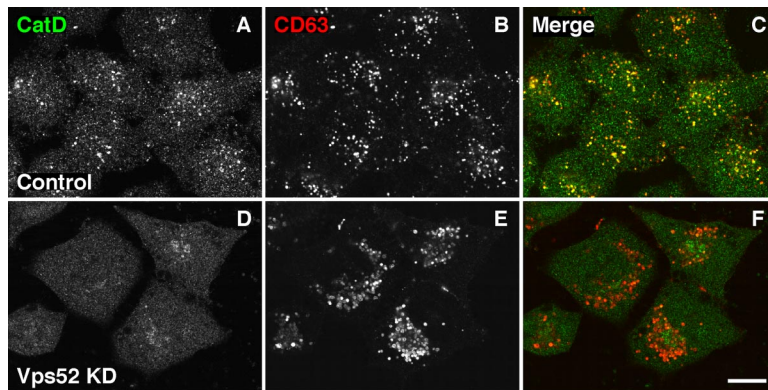
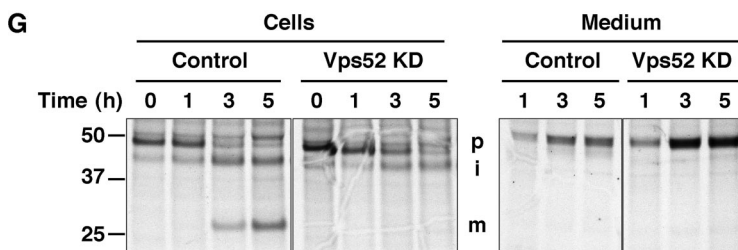


Figure 1. Depletion of *Vps52* causes missorting of *CatD*. HeLa cells grown on coverslips were transfected twice at 72-h intervals with siRNAs targeting 39 human proteins (SNX9, Rabex-5, Rabaptin-5, EEA1, Rab7, Rab9A, Rab6A, Rab6A', COG1, COG8, ARFRP1, ARL1, ARF6, GPP-130, GMx33, EpsinR, TGN46, Vps20, Vps30, Vps36, Vps39, Vps13, Vps52, Vps34, TMEM30A, TMEM30B, ATP8A1, ATP8A2, PIK-Fyve [PIP5K3], PIK3C2A, PIP5K3, PIK4CB, PI4KII, PIP5K1A, PIP5K1B, HPS3, HPS5, HPS6, UBE1L). At 72 h after the second round of transfection, the effects of siRNA treatment on the distribution of *CatD* were assessed by confocal immunofluorescence microscopy. Only control cells (A–C) and cells transfected with *Vps52* siRNA (D–F, knockdown: KD) are shown. Cells were double-labeled with antibodies to *CatD* (A and D, green channel) and to the lysosomal marker CD63 (B and E, red channel), followed by secondary antibodies. (C and F) Merged images, with yellow indicating colocalization. Bar, 10 μ m. (G). Pulse-chase analysis of *CatD* maturation in HeLa cells that were transfected twice at 72-h intervals with *Vps52* siRNA or with no siRNA (control). At 72 h after the second round of transfection, cells were metabolically labeled for 2 h at 20°C with [³⁵S]methionine-cysteine and chased for different periods at 37°C. Media and cell extracts were subjected to immunoprecipitation of *CatD* species. The immunoprecipitates were analyzed by SDS-PAGE and fluorography. The positions of the precursor (p), intermediate (i), and mature heavy chain (m) forms of *CatD* are indicated on the right. The positions of molecular mass markers (in kDa) are indicated on the left.



ture heavy chain (m) forms of *CatD* are indicated on the right. The positions of molecular mass markers (in kDa) are indicated on the left.

ments we concluded that the whole GARP complex is required for CatD sorting to lysosomes.

In yeast, the small GTPases Ypt6 and Arl1 have been shown to regulate the recruitment of the GARP complex to membranes (Siniosoglou and Pelham, 2001; Conibear *et al.*, 2003; Panic *et al.*, 2003). We observed that single depletion of the human orthologues of these proteins, Rab6A/A' (the siRNA oligonucleotides targeted both isoforms) and Arl1, slightly decreased processing and increased secretion of precursor CatD (Figure 2E). Combined depletion of Rab6A/A' and Arl1, however, exacerbated these defects, although in all cases they were less pronounced than those caused by depletion of GARP subunits (Figure 2E). These observations are consistent with the previously demonstrated role for Rab6A/A' and Arl1 in retrograde transport (Mallard *et al.*, 2002; Medigeshi and Schu, 2003; Lu *et al.*, 2004; Utskarpen *et al.*, 2006), which may be exerted through the recruitment of GARP and other protein tethers to membranes (Munro, 2005; Short *et al.*, 2005).

Localization of Human GARP to the TGN

Previous use of anti-peptide antibodies for immunofluorescence microscopy analyses showed that the endogenous GARP complex was localized to vesicles that were largely scattered throughout the cytoplasm and costained with endosomal markers (Liewen *et al.*, 2005). Some accumulation in the perinuclear area and colocalization with Golgi markers, however, was also noted (Liewen *et al.*, 2005). We sought to confirm this localization pattern, but unfortunately, our anti-peptide antibodies failed to immunostain endogenous GARP. To overcome this problem, we made a Vps54 construct that was tagged at the C-terminus with GFP, and expressed it by stable transfection into human H4 cells (Figure 3). Triple-labeling, immunofluorescence microscopy showed that this construct localized to a ribbon-like structure that coincided almost perfectly with the endogenous TGN marker, TGN46 (Figure 3). The structure containing Vps54-GFP also aligned with the Golgi cisternae stained for the marker protein, GM130, although merging of the images showed that the two structures were shifted relative to each other (Figure 3). Similar observations were made in HeLa cells expressing Vps54-GFP (see Figure 9, B–D). A fraction of Vps54-GFP was also consistently found on small puncta distributed throughout the cytoplasm (Figure 3). This fraction may represent cytosolic protein and/or association with small vesicles. These observations thus indicated that human GARP is largely associated with the TGN.

Altered Distribution of MPRs Underlies CatD Missorting in GARP-depleted Cells

We next investigated how depletion of the TGN-associated GARP complex causes CatD missorting. Like other acid hydrolases, CatD is sorted by the transmembrane MPRs, which follow a cycling itinerary between the TGN and endosomes. Immunofluorescence microscopy showed that, in HeLa cells, the CI-MPR localized to a collection of cytoplasmic vesicles that were more concentrated in the juxtannuclear area (Figure 4A). As previously reported, many of these vesicles showed colocalization with SNX2 (data not shown), a component of the retromer complex that is involved in the retrieval of the CI-MPR from endosomes (Carlton *et al.*, 2004; Rojas *et al.*, 2007), and only a few overlapped with the TGN-localized TGN46 (Figure 4, A–D). This indicated that the steady-state distribution of the CI-MPR is skewed toward endosomes in these cells. Depletion of Vps52 caused a dramatic redistribution of both the CI-MPR and TGN46. In >95% of Vps52 siRNA-treated cells, the majority of the

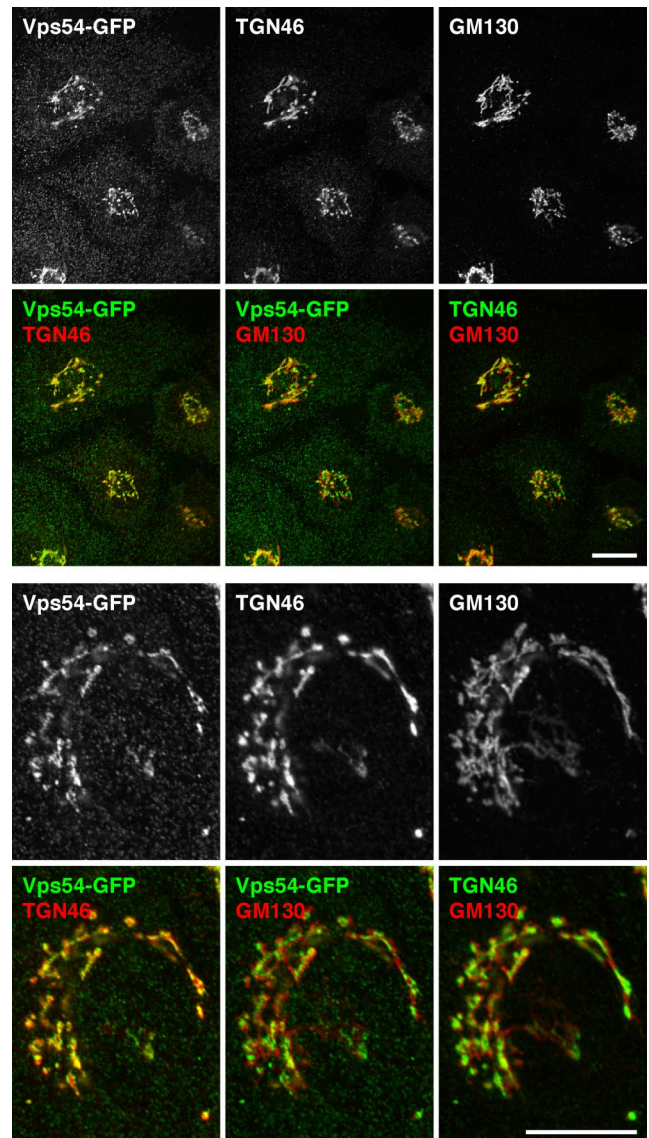


Figure 3. The GARP complex localizes to the TGN. H4 cells stably expressing a Vps54-GFP chimera were fixed in methanol, triple-labeled with antibodies to GFP (green), the TGN marker TGN46 (red/green), and the *cis*-Golgi marker GM-130 (red), followed by appropriate secondary antibodies, and examined by confocal immunofluorescence microscopy. Pairwise merging of images shows colocalization of Vps54-GFP with TGN46 (yellow) and segregation of these two proteins from the *cis*-Golgi marker GM-130. Bar, 10 μ m.

CI-MPR localized to a profusion of small vesicles scattered throughout the cytoplasm (Figure 4, E, I, and L; compare vesicle size in A and E insets), with the rest being found within a tight juxtannuclear structure (Figure 4E) that roughly colocalized with the Golgi cisternal marker, giantin (Figure 4G). To better characterize this juxtannuclear structure, we costained CI-MPR with the TGN marker p230 (Golgin-245) in Vps52-depleted cells (Figure 4, I–K). Merging of both images showed substantial overlap between the two signals (Figure 4K). We concluded from these experiments that this fraction of CI-MPR localizes to the TGN in GARP-depleted cells. A similar redistribution was observed for TGN46, with the notable difference that the total intensity of staining appeared substantially diminished (Figure 4F). This latter

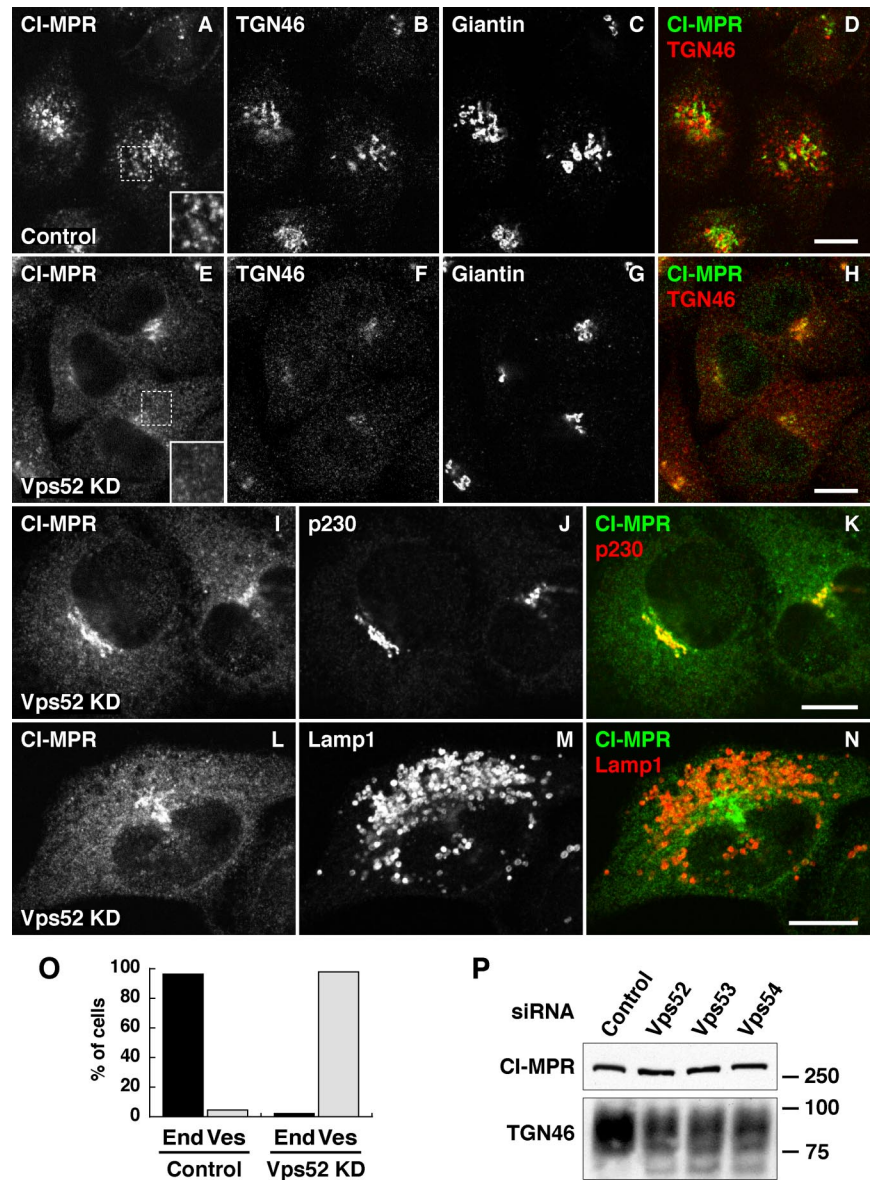


Figure 4. GARP depletion results in redistribution of the CI-MPR. (A–N) HeLa cells were transfected with siRNA directed to Vps52 (KD) or without siRNA (control) and analyzed by confocal immunofluorescence microscopy 72 h later (A–H) or 72 h after a second round of interference (I–N). Cells were fixed in methanol and labeled with antibodies to the indicated proteins followed by appropriate secondary antibodies. Bars, 10 μ m. (O). Quantification of the defects in CI-MPR distribution upon siRNA treatment. Three different samples, prepared as above, were inspected by epifluorescence microscopy and scored for either an endosomal or a Golgi/small vesicle appearance of CI-MPR ($n > 100$ cells per sample). The endosomal distribution corresponds to that of A, whereas the Golgi/small vesicle appearance corresponds to that of E, I, and L. (P). Levels of CI-MPR and TGN46 in GARP-depleted cells. HeLa cells were transfected twice at 24-h intervals with siRNAs directed to Vps52, Vps53, or Vps54, or without siRNA (control). At 48 h after the second round of transfection, equivalent amounts of lysates were subjected to SDS-PAGE and immunoblotting using rabbit polyclonal antibody to CI-MPR or sheep polyclonal antibody to TGN46. The positions of molecular mass (in kDa) markers are indicated on the right.

phenotype was quite dramatic and facilitated identification of GARP-depleted cells in subsequent experiments (for instance, see Figures 5, 8F, and 9, G and N). Immunoblot analysis showed that, unlike depletion of retromer components (Arighi *et al.*, 2004; Carlton *et al.*, 2004; Seaman, 2004; Rojas *et al.*, 2007), depletion of GARP subunits did not decrease the levels of the CI-MPR (Figure 4P). In contrast to the CI-MPR, and in agreement with the immunofluorescence microscopy results (Figure 4F), total TGN46 levels were decreased about fourfold by GARP depletion (Figure 4P).

The distribution of other TGN markers such as golgin-97 (data not shown) and Golgi cisternae markers such as giantin (Figure 4G) and GM130 and galactosyl transferase (data not shown) was unaffected by GARP depletion, indicating that the altered distribution of the CI-MPR and TGN46 was not due to global disruption of the Golgi complex. In addition, the transmembrane proteins, Lamp-1 (Figure 4M) and CD63 (Figure 1E), still localized to lysosomes in GARP-depleted cells although, as previously mentioned, the lysosomes appeared swollen and clustered in the juxtannuclear

area (Figures 1E and 4M) after prolonged depletion of GARP. Therefore, the absence of GARP causes specific defects in the distribution of transmembrane proteins such as the CI-MPR and TGN46 that cycle between the TGN and endosomes, as well as luminal cargo proteins such as CatD, which relies on the CI-MPR for trafficking.

Phenotypic Rescue of Vps52-depleted Cells by Transfection with siRNA-resistant Vps52 cDNA

To ascertain the specificity of the effects observed upon depletion of GARP subunits, we performed rescue experiments in which the RNAi-treated cells were transfected with siRNA-resistant cDNAs. After two rounds of treatment with siRNAs, cells were transfected with the corresponding cDNAs and analyzed 24 h later. Use of this protocol for Vps52 resulted in almost complete (>90% of transfected cells) rescue of the steady-state localization of CatD, CI-MPR, and TGN46 over a wide range of expression levels of the transfected construct (Figure 5). Similar results were obtained for depletion and rescue of Vps53 and Vps54 (data not shown).

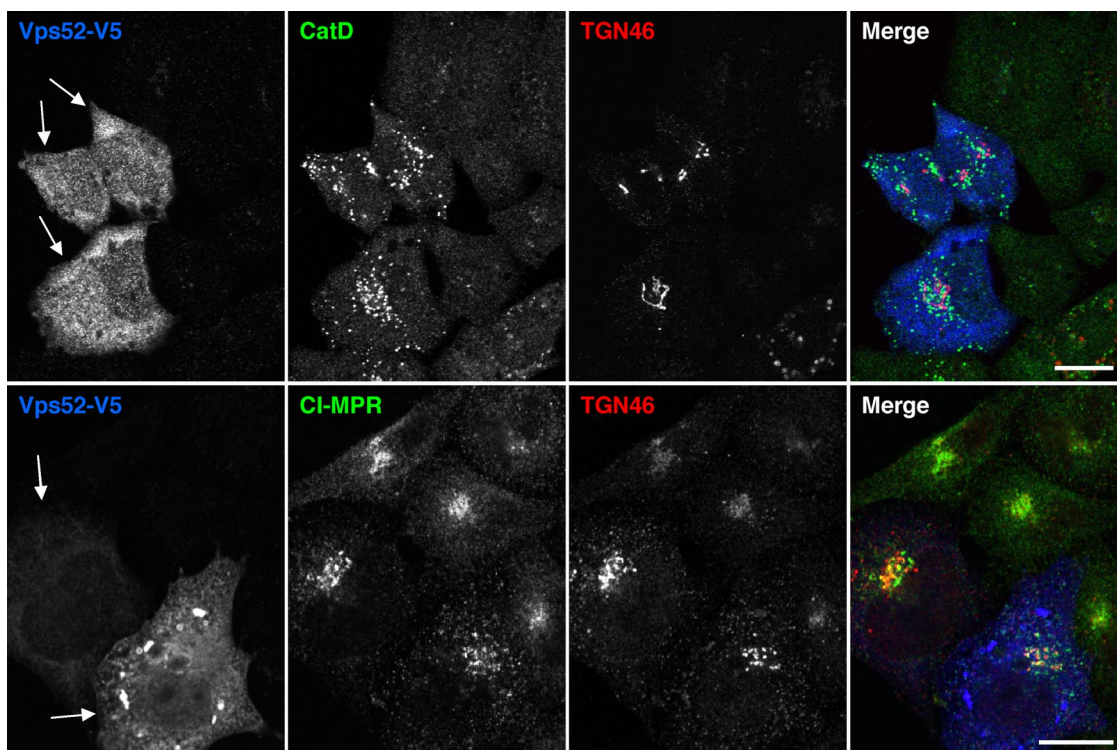


Figure 5. Rescue of CatD, TGN46, and CI-MPR localization by expression of siRNA-resistant Vps52. HeLa cells were transfected twice at 72-h intervals with siRNA directed to Vps52. At 24 h after the second transfection, cells were seeded on coverslips and transfected the following day with a plasmid encoding siRNA-resistant Vps52-V5. Cells were fixed 24 h after this final transfection, triple-labeled with antibodies to the indicated proteins followed by secondary antibodies and analyzed by confocal immunofluorescence microscopy. Notice that the normal localization of TGN46, CI-MPR, and CatD was recovered only in those cells expressing siRNA-resistant Vps52 (arrows). Bars, 10 μ m.

These results demonstrated that the protein localization defects observed in GARP-depleted cells were truly due to the absence of functional GARP and not to off-target effects.

Accumulation of CI-MPR in a Light Membrane Fraction in Vps52-depleted Cells

To further characterize the compartment where the CI-MPR accumulates in Vps52-depleted cells, we performed subcellular fractionation of disrupted HeLa cells by sedimentation on glycerol gradients (Figure 6). In control cells, a population of CI-MPR was found at the bottom of the gradient (fractions 11 and 12), which contained a mixture of Golgi (marked by GS28), endosomes (transferrin receptor), lysosomes (Lamp-2), and ER (BiP; Figure 6). Another CI-MPR population was found in lighter fractions that may correspond to transport intermediates. Interestingly, depletion of Vps52 caused a shift of a substantial fraction of the CI-MPR from heavy to lighter fractions that did not contain Golgi or endosomal markers but contained increased levels of the Vti1a, a t-SNARE that also cycles between the TGN and endosomes, and a fraction of the remaining TGN46 (Figure 6). These observations indicated that, in the absence of Vps52, the CI-MPR accumulates in a distinct, light membrane fraction that likely corresponds to the small vesicles visualized by immunofluorescence microscopy (Figure 4, E, I, and L).

Defective Trafficking of Internalized MPRs in Cells Depleted of Vps52

The yeast GARP complex has been proposed to function as a tethering complex that enables docking and fusion of endosome-derived, retrograde vesicles with the TGN

(Conibear and Stevens, 2000; Siniouoglou and Pelham, 2001; Whyte and Munro, 2002; Conibear *et al.*, 2003). To determine whether the altered steady-state distribution of the CI-MPR in Vps52-depleted human cells was due to a defect in retrograde transport, we examined the fate of antibody to the luminal domain of the CI-MPR that was internalized from the cell surface at steady state (Waguri *et al.*, 2003). Live control or Vps52-depleted HeLa cells were incubated for 1 h in the continuous presence of antibody to the CI-MPR, chased for 1 h in complete medium, fixed, permeabilized, and processed for immunofluorescence microscopy. In control cells, the internalized CI-MPR antibody exhibited a staining pattern (Figure 7, A and G) that was similar to that of the steady-state CI-MPR (Figures 4A and 7H), namely, juxtanuclear foci and vesicles that exhibited significant colocalization with SNX2 (Figure 7B). In Vps52-depleted cells, on the other hand, the internalized CI-MPR antibody accumulated in myriad small vesicles (Figure 7, D and J; 87% of Vps52 depleted cells showed this phenotype) similar to those containing the CI-MPR at steady state (Figures 4, E, I, and L, and 7K) and largely devoid of SNX2 (Figure 7, E and F). The similar distributions of internalized and total CI-MPR in both control cells (Figure 7, G–I) and Vps52-depleted cells (Figure 7, J–L), confirm that the mislocalization of CI-MPR in Vps52-depleted cells reflects changes in recycling and not biosynthetic sorting. A shorter pulse without a chase showed significant localization of internalized CI-MPR with SNX2 even in Vps52-depleted cells (Figure 7, M–O), indicating that the small vesicles represent a down-

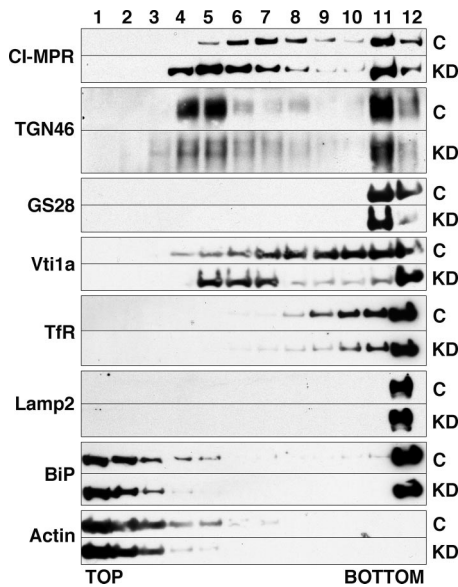


Figure 6. Subcellular fractionation shows that the CI-MPR accumulates in a light membrane fraction in *Vps52*-depleted cells. HeLa cells grown on 60-mm plates were transfected twice at 24-h intervals with siRNA directed to *Vps52* (KD) or without siRNA (control; C). Post-nuclear supernatants from both cell types were prepared 48 h after the second round of transfection, loaded on top of a 10–30% glycerol gradient, and analyzed by sedimentation velocity. The distribution of the CI-MPR, along with that of different organellar markers (TGN-localized TGN46, endosomal TfR and Vti1a, *cis*-Golgi SNARE GS28, lysosomal protein Lamp2, ER resident BiP, and cytosolic actin) was analyzed by immunoblotting of gradient fractions. Fraction 1 corresponds to the top of the gradient. Notice that both CI-MPR and Vti1a accumulate in lighter fractions in GARP-depleted cells.

stream compartment that is accessible by retrograde transport from the plasma membrane and endosomes. We interpret that accumulation of CI-MPR in this compartment (Figure 7, D and J) prevents it from assuming its normal steady-state distribution to endosomes (Figure 7, A and G). On the basis of the localization of human GARP to the TGN and the function of yeast GARP in mediating docking and fusion with the TGN (Conibear and Stevens, 2000; Sinioglou and Pelham, 2001; Conibear *et al.*, 2003), we think that the small vesicles correspond to endosome-to-TGN intermediates that are prevented from delivering retrograde cargo to the TGN by the absence of GARP.

Inhibition of Retrograde Transport of Shiga Toxin in Cells Depleted of Vps52

Because the CI-MPR retrieved from the cell surface does not simply stay at the TGN but rapidly exits toward endosomes, we sought to examine the effect of GARP depletion on retrograde transport of another cargo that does not follow this cycling pathway. The B-subunit of STxB is often used as a model cargo in studies of endosome-to-TGN transport (Mallard and Johannes, 2003). STxB is internalized from the cell surface and then undergoes retrograde transport using clathrin, retromer, and other machinery components common to various recycling cargoes (Tai *et al.*, 2004, 2005; Bujny *et al.*, 2007; Popoff *et al.*, 2007). Unlike the CI-MPR, however, STxB does not recycle back to endosomes but continues its retrograde path to the endoplasmic reticulum (ER; Mallard and Johannes, 2003). We observed that 1 h after internalization of the probe, the majority (~65%) of control cells

showed Cy3-conjugated STxB staining in a ribbon-like structure typical of the Golgi complex (Figure 8, A and B). In virtually all *Vps52*-depleted cells, in contrast, none of the internalized Cy3-conjugated STxB localized to the Golgi ribbon but instead remained in a population of small cytoplasmic vesicles (Figure 8, C and D). Rescue with RNAi-resistant, V5-tagged *Vps52* restored STxB transport to the Golgi complex (Figure 8, E and H; ~80% of transfected cells recovered the Golgi pattern for STxB). These observations confirmed that depletion of a GARP subunit blocks retrograde transport to the TGN and results in the accumulation of cargo in a vesicular compartment.

The Vps54 Wobbler Mutant Is Incorporated into the GARP Complex and Retains Function in Sorting

A single point mutation near the C-terminus of *Vps54* (L967Q) causes the Wobbler phenotype in the mouse, which is characterized by defects in motor neuron function and male sterility (Schmitt-John *et al.*, 2005). Complete ablation of the *Vps54* gene, however, is lethal at day 12.5 of embryonic development (Schmitt-John *et al.*, 2005). This indicates that the Wobbler mutation is hypomorphic. To investigate the effects of this mutation on the function of the GARP complex, we initially examined the assembly of V5-tagged *Vps54*(L967Q) in transfected cells. We observed that, although this mutant protein was expressed at levels lower than those of the wild-type protein, it nonetheless assembled with *Vps52* and *Vps53* (Figure 9A). We took advantage of this assay to determine what part of *Vps54* assembled with the other two subunits. To this end, we expressed V5-tagged forms of *Vps54*(1-515) and *Vps54*(535-977), comprising the N- and C-terminal portions of *Vps54*, respectively. We found that it was the N-terminal part that assembled into the GARP complex (Figure 9A), a finding that was consistent with the ability of the C-terminally mutated Wobbler allele to be incorporated into the complex. Moreover, immunofluorescence microscopy analysis of cells transfected with GFP-tagged *Vps54*(L967Q) Wobbler mutant showed that this protein localized to the TGN (Figure 9, E–G). Finally, transfection of *Vps54*-depleted cells with RNAi-resistant *Vps54*(L967Q)-V5 or *Vps54*(L967Q)-GFP restored the normal distribution of CatD, TGN46, and CI-MPR within cells (Figure 9, H–O). Thus, the *Vps54* Wobbler mutant appears to retain activity in trafficking between endosomes and the TGN.

DISCUSSION

The results presented here indicate that the mammalian GARP complex is required for the trafficking of CatD to lysosomes by enabling the recycling of the CI-MPR from endosomes to the TGN. In the absence of GARP, the CI-MPR accumulates in a population of small vesicles downstream of endosomes. The ensuing depletion of MPRs from the TGN causes newly synthesized CatD to be released into the extracellular medium as an uncleaved precursor instead of being sorted to endosomes and then to lysosomes. Loss of CatD, and likely of other mannose 6-phosphate-modified hydrolases, results in swelling of the lysosomes, a phenotype similar to that of lysosomal storage disorders.

Where does GARP act in this process? A previous study had suggested a mostly endosomal localization for mammalian GARP (Liewen *et al.*, 2005). However, our analyses of H4 and HeLa cells expressing *Vps54*-GFP indicate that GARP is mainly associated with the TGN (Figures 3 and 9, B–D). It is then at this location that GARP must participate in CI-MPR trafficking. On the basis of the proposed function of yeast GARP (Conibear and Stevens, 2000; Sinioglou and Pelham, 2001, 2002; Whyte and Munro, 2002; Conibear *et al.*,

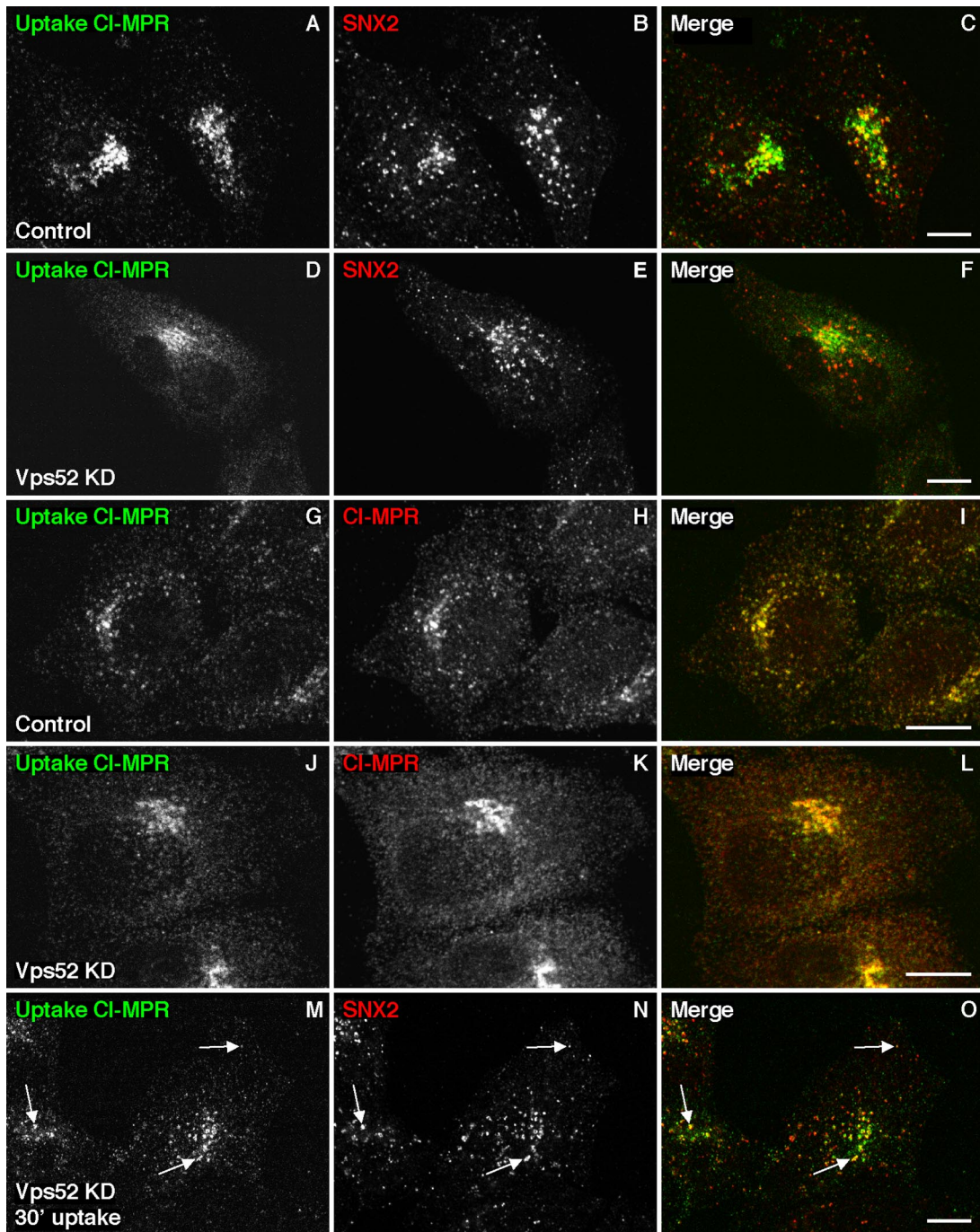


Figure 7. Defective trafficking of internalized CI-MPR in *Vps52*-depleted cells. Live control cells (A–C and G–I) or cells depleted of *Vps52* for 72 h (D–F and J–L) were incubated in the continuous presence of mAb to the luminal domain of CI-MPR for 1 h at 37°C and then washed and chased for another hour in complete medium before fixation and analysis by immunofluorescence microscopy. Notice that GARP-depleted cells accumulated small vesicles containing internalized CI-MPR (D and J) that were distinct from endosomes positive for the early endosomal marker SNX2 (E). (M–O) GARP-depleted cells were incubated with antibody to CI-MPR for only 30 min without further chase. Significant colocalization between internalized CI-MPR and SNX2 was observed under these conditions (arrows). Bars, 10 μ m.

2003; Panic *et al.*, 2003), we think that mammalian GARP is involved in the tethering or docking of endosome-derived, retrograde transport carriers to the TGN. This would be followed by SNARE-mediated fusion and delivery of the CI-MPR into the TGN. Indeed, depletion of GARP causes a shift in the steady-state distribution of the CI-MPRs from a set of relatively large endosomal structures to myriad small

vesicles scattered throughout the cytoplasm (Figure 4, E, I, and L). A similar accumulation in small vesicles is observed for CI-MPR internalized from the plasma membrane (Figure 7, D and J), indicating that these vesicles lie in the retrograde transport pathway. The small vesicles are lighter than endosomes or the Golgi complex (Figure 6) and lack markers of either of these organelles (Figure 4). Importantly, they do

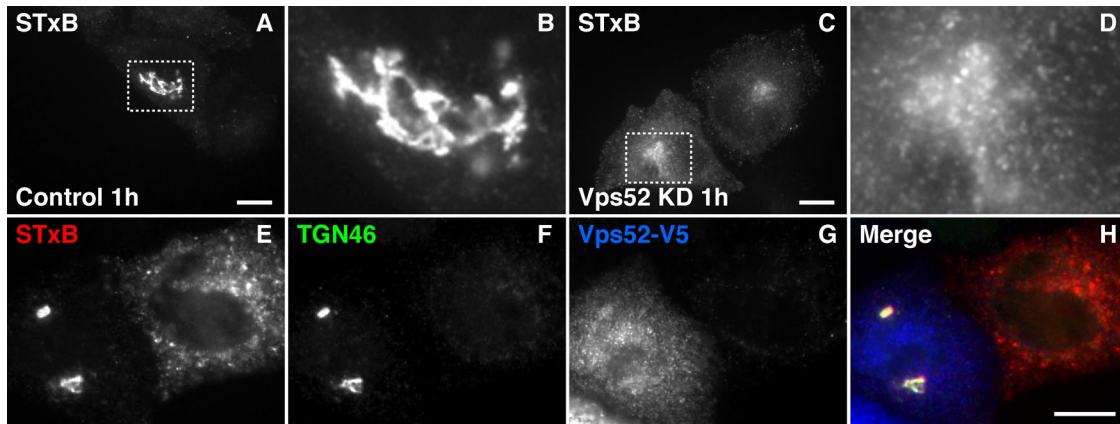


Figure 8. Defective retrograde trafficking of Shiga toxin B subunit in Vps52-depleted cells. HeLa cells were transfected twice at 24-h intervals with siRNA directed to Vps52 (KD; C and D) or without siRNA (control; A and B). The effects of Vps52 depletion on the retrograde trafficking of STxB were assessed by epifluorescence microscopy 72 h after the initial transfection. Live cells were incubated at 37°C with 0.5 $\mu\text{g/ml}$ Cy3-STxB for 15 min and chased in complete medium for 60 min before being fixed in paraformaldehyde and analyzed by immunofluorescence microscopy. Notice that STxB is efficiently transported to the Golgi complex in mock-treated cells (A, enlarged in B) but remains in small vesicles in Vps52-depleted cells (C, enlarged in D). In E–H, Vps52-depleted cells were transfected with a plasmid encoding siRNA-resistant Vps52-V5 for 16 h before incubation with STxB-containing medium under the same conditions. Fixed cells were labeled with antibodies to the indicated proteins followed by secondary antibodies. Notice that expression of Vps52-V5 rescues retrograde trafficking of STxB to the Golgi complex. Bars, 10 μm .

not contain SNX2 (Figure 7E), a component of the retromer complex that initiates the retrieval of the CI-MPR from endosomes by diverting the receptor into recycling tubules. Moreover, internalized CI-MPR passes through SNX2-positive endosomes before accumulating in the small vesicles (Figure 7, M–O). This places the small vesicles past the tubular endosomal network (TEN; Bonifacino and Rojas, 2006) through which the CI-MPR transits en route to the TGN (Arighi *et al.*, 2004). Thus, the small vesicles are likely intermediates in the transport between the TEN and the TGN.

Interestingly, the levels of CI-MPR are not changed by depletion of GARP despite its altered distribution (Figure 4P). This is in contrast to the depletion of retromer, which results in lower levels of CI-MPR due to its diversion to lysosomes (Arighi *et al.*, 2004). This indicates that the small vesicles where the CI-MPR accumulates in the absence of GARP are past the point where default transport to lysosomes is possible.

The role of GARP in retrograde transport is not limited to CI-MPR trafficking because the recycling TGN protein, TGN46, and the bacterial toxin, STxB, are also prevented from reaching the TGN in GARP-depleted cells. In these cells, both TGN46 (Figure 4F) and internalized STxB (Figure 8, C and D) accumulate in small vesicles similar to those that contain the CI-MPR. However, some differences with the behavior of the CI-MPR are apparent. The total levels of TGN46 are decreased (Figure 4P). In addition, STxB also accumulates in larger structures that colocalize with endosomal markers (Figure 8 and data not shown). This suggests that some cargo proteins back up into endosomal compartments in the absence of GARP. Despite these differences, it is clear that GARP is required for the retrograde transport of different types of protein: recycling transmembrane proteins like the CI-MPR and TGN46, and a glycosphingolipid-binding luminal protein like STxB. GARP thus appears to function as a general mediator of retrograde transport to the TGN.

Previous studies have identified other proteins that function to tether retrograde transport intermediates to the TGN. Among these are the golgins, golgin-97 (Lu *et al.*, 2004), golgin-245 (Yoshino *et al.*, 2005), GCC88 (Lieu *et al.*, 2007),

and GCC185 (Reddy *et al.*, 2006; Derby *et al.*, 2007). It is currently unclear why so many tethering factors would be involved in retrograde transport. One possibility is that they all cooperate to dock the same set of retrograde transport carriers to the TGN. An alternative possibility is that each participates in the docking of a different type of carrier, as defined by its origin or cargo. For example, GCC185 participates, together with Rab9 and TIP47, in retrieval of CI-MPR specifically from late endosomes (Reddy *et al.*, 2006). Another variation is exemplified by GCC88, which participates in retrograde transport of CI-MPR and TGN38 (the rat ortholog of human TGN46), but not STxB (Lieu *et al.*, 2007). This is consistent with the existence of multiple routes and carriers for retrograde transport. To the extent that we have analyzed it, the role of GARP appears to be general to various cargo proteins.

Although most of the CI-MPR accumulates in small vesicles in GARP-depleted cells, a fraction appears to concentrate in a juxtannuclear structure that colocalizes with Golgi markers (Figure 4, I–K). This may indicate that some CI-MPR molecules are still delivered to the TGN in the absence of GARP, perhaps due to the action of the other tethering factors mentioned above. Alternatively, the juxtannuclear remnant may reflect a certain degree of inhibition of exit from the Golgi complex. Indeed, after prolonged (≥ 5 d) depletion of GARP, we observed that even the plasma-membrane-targeted VSV-G protein accumulates to some extent in the Golgi complex. This could point to an additional role of GARP in export from the Golgi complex. In this regard, interference with another tethering factor, golgin-97, has been shown to inhibit transport of the adhesion molecule, E-cadherin, from the Golgi complex to the basolateral surface of polarized epithelial cells (Lock *et al.*, 2005). However, accumulation in the Golgi complex could also be secondary to impaired retrieval of factors that are required for exit from the TGN, as has been previously proposed for yeast GARP (Conibear and Stevens, 2000).

As would be expected for a complex that plays a general role in retrograde transport, GARP is essential for embryonic development and viability in the mouse (Schmitt-John *et al.*,

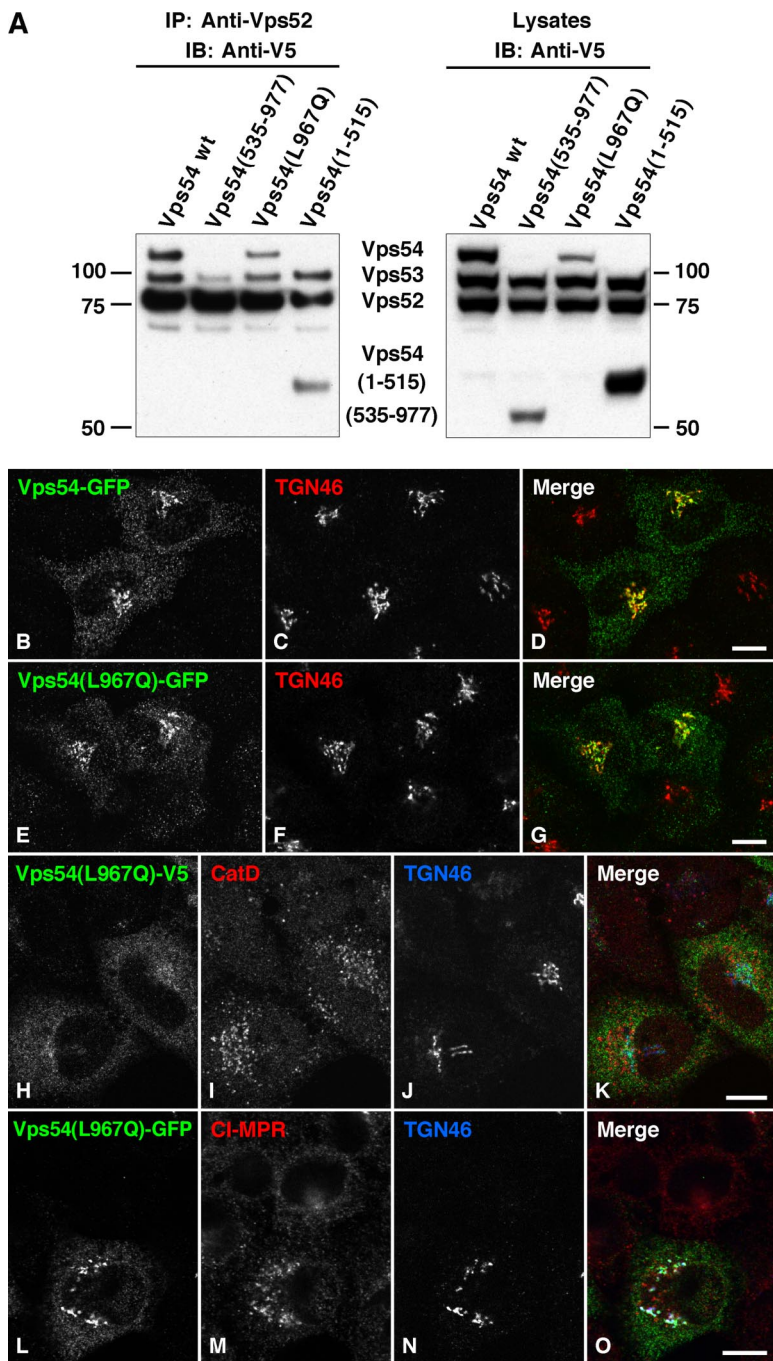


Figure 9. The Vps54 Wobbler mutant protein is incorporated into the GARP complex and is functional in sorting. (A) The Wobbler mutant protein, Vps54(L967Q), and the N-terminal domain, Vps54(1-515), but not the C-terminal domain, Vps54(535-977), assemble into the GARP complex. HeLa cells grown on six-well plates were transiently transfected with combinations of plasmids encoding Vps52-V5, Vps53-V5, and the Vps54-V5 forms indicated at the top. At 24 h after transfection, proteins were extracted in 1% Triton X-100 and subjected to immunoprecipitation with antibody to Vps52. Immunoprecipitates were analyzed by SDS-PAGE and immunoblotting with antibody to the V5 epitope (left panel). Ten percent of the total lysates was analyzed in parallel (right panel). (B-G). Localization of wild-type Vps54-GFP and the Wobbler mutant Vps54(L967Q)-GFP to the TGN. HeLa cells were transfected with plasmids encoding wild type (B-D) or Wobbler mutant (E and F) alleles of Vps54-GFP, fixed in methanol 24 h after transfection, double-labeled with antibodies to GFP and TGN46, and analyzed by confocal immunofluorescence microscopy. (H-O) The Wobbler mutant proteins Vps54(L967Q)-V5 and Vps54(L967Q)-GFP are able to restore the normal localization of CatD, CI-MPR, and TGN46. HeLa cells depleted of Vps54 were transfected with plasmids encoding siRNA-resistant Vps54(L967Q)-V5 (H-K) or Vps54(L967Q)-GFP (L-O), fixed in methanol 16 h later, triple-labeled with antibodies to the indicated proteins, followed by secondary antibodies, and analyzed by confocal immunofluorescence microscopy. Bars, 10 μ m.

2005). Mouse embryos with homozygous disruption of the *Vps54* gene fail to thrive and die at about day 12.5 postcoitum (Schmitt-John *et al.*, 2005). However, the mutant Wobbler mouse, which carries the missense mutation L967Q in Vps54 (Schmitt-John *et al.*, 2005), is viable though it exhibits motor neuron degeneration similar to that of amyotrophic lateral sclerosis (Boillee *et al.*, 2003). The different phenotypes of the Vps54 disruption and Wobbler mutants are likely explained by the ability of the Vps54(L967Q) mutant protein to assemble with the other subunits of GARP and to support sorting of CI-MPR, CatD, and TGN46 (Figure 9). The expression levels of Vps54(L967Q), however, are lower than those of its wild-type counterpart (Figure 9A), perhaps explaining the Wobbler motor neuron defect.

The demonstration of a role of the human GARP complex in retrograde transport further supports the notion that the core machinery for acid hydrolase sorting has been faithfully conserved from yeast to humans, to the point of utilizing similar proteins or complexes at virtually every step of the sorting pathways. This conservation undoubtedly stems from the essential nature of endosomal transport pathways and, in particular, retrograde transport from endosomes to the TGN for the maintenance of cellular homeostasis.

ACKNOWLEDGMENTS

We thank X. Zhu and H.-I. Tsai for expert technical assistance, L. Johannes for Cy3-STxB, M. Marks (University of Pennsylvania, Philadelphia, PA) for an-

tibody to p230, and J. G. Magadán for critical review of the manuscript. This work was funded by the Intramural Program of National Institute of Child Health and Human Development, National Institutes of Health. F.J.P.-V. is the recipient of a postdoctoral fellowship from the Ministerio de Educación y Ciencia of Spain.

REFERENCES

- Arighi, C. N., Hartnell, L. M., Aguilar, R. C., Haft, C. R., and Bonifacino, J. S. (2004). Role of the mammalian retromer in sorting of the cation-independent mannose 6-phosphate receptor. *J. Cell Biol.* *165*, 123–133.
- Boillee, S., Peschanski, M., and Junier, M. P. (2003). The wobbler mouse: a neurodegeneration jigsaw puzzle. *Mol. Neurobiol.* *28*, 65–106.
- Bonifacino, J. S. (2004). The GGA proteins: adaptors on the move. *Nat. Rev. Mol. Cell Biol.* *5*, 23–32.
- Bonifacino, J. S., and Rojas, R. (2006). Retrograde transport from endosomes to the trans-Golgi network. *Nat. Rev. Mol. Cell Biol.* *7*, 568–579.
- Bowers, K., and Stevens, T. H. (2005). Protein transport from the late Golgi to the vacuole in the yeast *Saccharomyces cerevisiae*. *Biochim. Biophys. Acta* *1744*, 438–454.
- Bujny, M. V., Popoff, V., Johannes, L., and Cullen, P. J. (2007). The retromer component sorting nexin-1 is required for efficient retrograde transport of Shiga toxin from early endosome to the trans Golgi network. *J. Cell Sci.* *120*, 2010–2021.
- Carlton, J., Bujny, M., Peter, B. J., Oorschot, V. M., Rutherford, A., Mellor, H., Klumperman, J., McMahon, H. T., and Cullen, P. J. (2004). Sorting nexin-1 mediates tubular endosome-to-TGN transport through coincidence sensing of high-curvature membranes and 3-phosphoinositides. *Curr. Biol.* *14*, 1791–1800.
- Carlton, J., Bujny, M., Rutherford, A., and Cullen, P. (2005a). Sorting nexins—unifying trends and new perspectives. *Traffic* *6*, 75–82.
- Carlton, J. G., Bujny, M. V., Peter, B. J., Oorschot, V. M., Rutherford, A., Arkell, R. S., Klumperman, J., McMahon, H. T., and Cullen, P. J. (2005b). Sorting nexin-2 is associated with tubular elements of the early endosome, but is not essential for retromer-mediated endosome-to-TGN transport. *J. Cell Sci.* *118*, 4527–4539.
- Carroll, K. S., Hanna, J., Simon, I., Krise, J., Barbero, P., and Pfeffer, S. R. (2001). Role of Rab9 GTPase in facilitating receptor recruitment by TIP47. *Science* *292*, 1373–1376.
- Conibear, E., Cleck, J. N., and Stevens, T. H. (2003). Vps51p mediates the association of the GARP (Vps52/53/54) complex with the late Golgi t-SNARE Tlg1p. *Mol. Biol. Cell* *14*, 1610–1623.
- Conibear, E., and Stevens, T. H. (2000). Vps52p, Vps53p, and Vps54p form a novel multisubunit complex required for protein sorting at the yeast late Golgi. *Mol. Biol. Cell* *11*, 305–323.
- Derby, M. C., Lieu, Z. Z., Brown, D., Stow, J. L., Goud, B., and Gleeson, P. A. (2007). The trans-Golgi network golgin, GCC185, is required for endosome-to-Golgi transport and maintenance of Golgi structure. *Traffic* *8*, 758–773.
- Diaz, E., and Pfeffer, S. R. (1998). TIP47, a cargo selection device for mannose 6-phosphate receptor trafficking. *Cell* *93*, 433–443.
- Ghosh, P., Griffith, J., Geuze, H. J., and Kornfeld, S. (2003). Mammalian GGAs act together to sort mannose 6-phosphate receptors. *J. Cell Biol.* *163*, 755–766.
- Ghosh, P., and Kornfeld, S. (2004). The GGA proteins: key players in protein sorting at the trans-Golgi network. *Eur. J. Cell Biol.* *83*, 257–262.
- Ghosh, R. N., Mallet, W. G., Soe, T. T., McGraw, T. E., and Maxfield, F. R. (1998). An endocytosed TGN38 chimeric protein is delivered to the TGN after trafficking through the endocytic recycling compartment in CHO cells. *J. Cell Biol.* *142*, 923–936.
- Haft, C. R., de la Luz Sierra, M., Bafford, R., Lesniak, M. A., Barr, V. A., and Taylor, S. I. (2000). Human orthologs of yeast vacuolar protein sorting proteins Vps26, 29, and 35, assembly into multimeric complexes. *Mol. Biol. Cell* *11*, 4105–4116.
- Kametaka, S., Mattera, R., and Bonifacino, J. S. (2005). Epidermal growth factor-dependent phosphorylation of the GGA3 adaptor protein regulates its recruitment to membranes. *Mol. Cell Biol.* *25*, 7988–8000.
- Kornfeld, S., and Mellman, I. (1989). The biogenesis of lysosomes. *Annu. Rev. Cell Biol.* *5*, 483–525.
- Lazzarino, D. A., and Gabel, C. A. (1988). Biosynthesis of the mannose 6-phosphate recognition marker in transport-impaired mouse lymphoma cells. Demonstration of a two-step phosphorylation. *J. Biol. Chem.* *263*, 10118–10126.
- Lieu, Z. Z., Derby, M. C., Teasdale, R. D., Hart, C., Gunn, P., and Gleeson, P. A. (2007). The golgin, GCC88, is required for efficient retrograde transport of cargo from the early endosomes to the trans-Golgi network. *Mol. Biol. Cell* *18*, 4979–4991.
- Liewen, H., Meinhold-Heerlein, I., Oliveira, V., Schwarzenbacher, R., Luo, G., Wadle, A., Jung, M., Pfreundschuh, M., and Stenner-Liewen, F. (2005). Characterization of the human GARP (Golgi associated retrograde protein) complex. *Exp. Cell Res.* *306*, 24–34.
- Lock, J. G., Hammond, L. A., Houghton, F., Gleeson, P. A., and Stow, J. L. (2005). E-cadherin transport from the trans-Golgi network in tubulovesicular carriers is selectively regulated by golgin-97. *Traffic* *6*, 1142–1156.
- Lu, L., Tai, G., and Hong, W. (2004). Autoantigen Golgin-97, an effector of Arl1 GTPase, participates in traffic from the endosome to the trans-Golgi network. *Mol. Biol. Cell* *15*, 4426–4443.
- Mallard, F., and Johannes, L. (2003). Shiga toxin B-subunit as a tool to study retrograde transport. *Methods Mol. Med.* *73*, 209–220.
- Mallard, F., Tang, B. L., Galli, T., Tenza, D., Saint-Pol, A., Yue, X., Antony, C., Hong, W., Goud, B., and Johannes, L. (2002). Early/recycling endosomes-to-TGN transport involves two SNARE complexes and a Rab6 isoform. *J. Cell Biol.* *156*, 653–664.
- Mardones, G. A., Burgos, P. V., Brooks, D. A., Parkinson-Lawrence, E., Mattera, R., and Bonifacino, J. S. (2007). The trans-Golgi network accessory protein p56 promotes long-range movement of GGA/clathrin-containing transport carriers and lysosomal enzyme sorting. *Mol. Biol. Cell* *18*, 3486–3501.
- Medigeschi, G. R., and Schu, P. (2003). Characterization of the in vitro retrograde transport of MPR46. *Traffic* *4*, 802–811.
- Munro, S. (2005). The Arf-like GTPase Arl1 and its role in membrane traffic. *Biochem. Soc. Trans.* *33*, 601–605.
- Panic, B., Whyte, J. R., and Munro, S. (2003). The ARF-like GTPases Arl1p and Arl3p act in a pathway that interacts with vesicle-tethering factors at the Golgi apparatus. *Curr. Biol.* *13*, 405–410.
- Popoff, V., Mardones, G. A., Tenza, D., Rojas, R., Lamaze, C., Bonifacino, J. S., Raposo, G., and Johannes, L. (2007). The retromer complex and clathrin define an early endosomal retrograde exit site. *J. Cell Sci.* *120*, 2022–2031.
- Reddy, J. V., Burguete, A. S., Sridevi, K., Ganley, I. G., Nottingham, R. M., and Pfeffer, S. R. (2006). A functional role for the GCC185 golgin in mannose 6-phosphate receptor recycling. *Mol. Biol. Cell* *17*, 4353–4363.
- Reggiori, F., Wang, C. W., Stromhaug, P. E., Shintani, T., and Klionsky, D. J. (2003). Vps51 is part of the yeast Vps fifty-three tethering complex essential for retrograde traffic from the early endosome and Cvt vesicle completion. *J. Biol. Chem.* *278*, 5009–5020.
- Rohrer, J., and Kornfeld, R. (2001). Lysosomal hydrolase mannose 6-phosphate uncovering enzyme resides in the trans-Golgi network. *Mol. Biol. Cell* *12*, 1623–1631.
- Rojas, R., Kametaka, S., Haft, C. R., and Bonifacino, J. S. (2007). Interchangeable but essential functions of SNX1 and SNX2 in the association of retromer with endosomes and the trafficking of mannose 6-phosphate receptors. *Mol. Cell Biol.* *27*, 1112–1124.
- Saint-Pol, A. *et al.* (2004). Clathrin adaptor epsinR is required for retrograde sorting on early endosomal membranes. *Dev. Cell* *6*, 525–538.
- Schmitt-John, T. *et al.* (2005). Mutation of Vps54 causes motor neuron disease and defective spermiogenesis in the wobbler mouse. *Nat. Genet.* *37*, 1213–1215.
- Seaman, M. N. (2004). Cargo-selective endosomal sorting for retrieval to the Golgi requires retromer. *J. Cell Biol.* *165*, 111–122.
- Short, B., Haas, A., and Barr, F. A. (2005). Golgins and GTPases, giving identity and structure to the Golgi apparatus. *Biochim. Biophys. Acta* *1744*, 383–395.
- Siniosoglou, S., and Pelham, H. R. (2001). An effector of Ypt6p binds the SNARE Tlg1p and mediates selective fusion of vesicles with late Golgi membranes. *EMBO J.* *20*, 5991–5998.
- Siniosoglou, S., and Pelham, H. R. (2002). Vps51p links the VFT complex to the SNARE Tlg1p. *J. Biol. Chem.* *277*, 48318–48324.
- Tai, G., Lu, L., Johannes, L., and Hong, W. (2005). Functional analysis of Arl1 and golgin-97 in endosome-to-TGN transport using recombinant Shiga toxin B fragment. *Methods Enzymol.* *404*, 442–453.
- Tai, G., Lu, L., Wang, T. L., Tang, B. L., Goud, B., Johannes, L., and Hong, W. (2004). Participation of the syntaxin 5/Ykt6/GS28/GS15 SNARE complex in transport from the early/recycling endosome to the trans-Golgi network. *Mol. Biol. Cell* *15*, 4011–4022.

- Utskarpen, A., Slagsvold, H. H., Iversen, T. G., Walchli, S., and Sandvig, K. (2006). Transport of ricin from endosomes to the Golgi apparatus is regulated by Rab6A and Rab6A'. *Traffic* 7, 663–672.
- Waguri, S., Dewitte, F., Le Borgne, R., Rouille, Y., Uchiyama, Y., Dubremetz, J. F., and Hoflack, B. (2003). Visualization of TGN to endosome trafficking through fluorescently labeled MPR and AP-1 in living cells. *Mol. Biol. Cell* 14, 142–155.
- Whyte, J. R., and Munro, S. (2002). Vesicle tethering complexes in membrane traffic. *J. Cell Sci.* 115, 2627–2637.
- Yoshino, A., Setty, S. R., Poynton, C., Whiteman, E. L., Saint-Pol, A., Burd, C. G., Johannes, L., Holzbaur, E. L., Koval, M., McCaffery, J. M., and Marks, M. S. (2005). tGolgin-1 (p230, golgin-245) modulates Shiga-toxin transport to the Golgi and Golgi motility towards the microtubule-organizing centre. *J. Cell Sci.* 118, 2279–2293.
- Zolov, S. N., and Lupashin, V. V. (2005). Cog3p depletion blocks vesicle-mediated Golgi retrograde trafficking in HeLa cells. *J. Cell Biol.* 168, 747–759.